



On the role of inductive loops at low frequencies in PEM electrolysis

Niklas Hensle^{a,b,*}, Debora Brinker^b, Sebastian Metz^a, Tom Smolinka^a, André Weber^b

^a Fraunhofer Institute for Solar Energy Systems ISE, Heidenhofstrasse 2, 79110 Freiburg, Germany

^b Institute for Applied Materials (IAM-ET), Karlsruhe Institute of Technology (KIT), Adenauerring 20b, 76131 Karlsruhe, Germany

ARTICLE INFO

Keywords:

PEM electrolysis
EIS
Inductive loops
Low frequency
High current density
Negative polarization resistance

ABSTRACT

Inductive loops at low frequencies have been observed in the electrochemical impedance spectra (EIS) of various electrochemical cells. Although different physicochemical models for this phenomenon have been suggested in many other applications, this topic has not been widely discussed in the field of proton exchange membrane (PEM) electrolysis.

In this article, low-frequency inductive loops in PEM electrolysis cells and their impact on cell performance are analyzed. We show that this phenomenon is reproducible and occurs with different cell materials and setups. Its impact increases with increasing current density and decreasing temperature. At extreme conditions ($7 \text{ A}\cdot\text{cm}^{-2}$, 40°C) we show that the negative polarization resistance of the inductive process can exceed the capacitive polarization processes by a factor of three, resulting in a direct current resistance less than the high frequency series resistance of the cell.

1. Introduction

Inductive behavior at low frequencies in electrochemical impedance spectroscopy (EIS) is a phenomenon that has already been reported for a variety of electrochemical systems. It has, for example, been discussed in the fields of lithium-ion batteries [1–3], solid oxide cells (SOC) [4–8] and PEM fuel cells (PEMFC) [9–13], among others. Klotz [14] provides a comprehensive overview including several other applications.

Electrochemical cells often show an inductive semicircle at low frequencies. In general, inductive behavior is identified based on positive imaginary values in the Nyquist plot. Herein, the real part $\text{Re}(Z)$ decreases with decreasing frequency and the inductive polarization resistance of the related electrochemical process exhibits a negative value. Thus, the related polarization phenomena decrease the direct current (DC) resistance and hence improve the cell performance.

In the field of PEMFC, a number of hypotheses have been reported regarding the cause of inductive loops at low frequencies. These are the formation of platinum oxide at the surface and its dissolution [15], side reactions including adsorbed intermediates (e.g. hydrogen peroxide) [16] or slow water diffusion in the ionomer [15,17]. Most reports describe this inductive behavior using physicochemical models, equivalent circuit models (ECM) or Distribution of Relaxation Time (DRT) analysis [13,15,16,18,19]. Göhr and Schiller introduced an ECM to describe the relaxation impedance of interfaces, which typically shows

inductive behavior at low frequencies [20]. This model can be used to describe, for example, the carbon monoxide poisoning of the anode of a PEMFC [21,22].

To the best of our knowledge, no work dedicated to the analysis of low-frequency inductive behavior has been reported for PEM electrolysis cells (PEMEC). Most of the published articles on EIS in this field focus on the series resistance at high frequencies and on the capacitive loop at medium frequencies [23–28]. One of the very few reports that at least mentions low-frequency inductive behavior is provided by Ferriday and Middleton [29]. However, they describe EIS results in PEMEC for current densities $\leq 0.5 \text{ A}\cdot\text{cm}^{-2}$ in the low-frequency range only as “highly non-linear, non-reproducible” and provide no further characterization or analysis of what they call a “pseudo-inductive demeanor”.

In our opinion, the lack of reports on this inductive behavior is due to two factors. On the one hand, EIS is often not performed at low frequencies ($<100 \text{ mHz}$) due to long measurement times and the instability of the cell during the measurement. On the other hand, recent publications do not focus on EIS at high current densities ($>4 \text{ A}\cdot\text{cm}^{-2}$), which enhance the inductive processes.

In this article the low-frequency behavior of a number of PEMECs differing in cell components, cell housings and test benches is analyzed. We show that the inductive behavior is reproducible and by no means a measurement artefact. Comparison of the local slopes of polarization curves reveals that the negative polarization resistance of the inductive

* Corresponding author at: Fraunhofer Institute for Solar Energy Systems ISE, Heidenhofstrasse 2, 79110 Freiburg, Germany.

E-mail address: niklas.hensle@ise.fraunhofer.de (N. Hensle).

<https://doi.org/10.1016/j.elecom.2023.107585>

Received 26 July 2023; Received in revised form 13 September 2023; Accepted 14 September 2023

Available online 15 September 2023

1388-2481/© 2023 The Authors. Published by Elsevier B.V. This is an open access article under the CC BY-NC-ND license (<http://creativecommons.org/licenses/by-nc-nd/4.0/>).

polarization process improves the cell performance and thus should be considered in impedance-based performance analyses of PEMECs.

2. Experimental

A variety of materials were employed as catalyst-coated membranes (CCM) and porous transport layers (PTL), and different test cell housings and test benches were used in the measurements reported here. The measurements were conducted at two different laboratories at Fraunhofer ISE and KIT IAM-ET.

At Fraunhofer ISE, the ISE reference cell with an active area of 4 cm² [30] and a newly designed “along-the-channel” (AtC) cell with an active area of 60 cm² were used at a test bench developed in-house [31]. At KIT IAM-ET, a commercial EL10 cell from Schaeffler Technologies AG & Co. KG, Germany, with an active area of 10 cm² was used at a commercial E20 test bench from Greenlight Innovation, Canada. State-of-the-art CCMs from three different commercial suppliers are tested. Regarding PTL materials, different combinations of coated and uncoated titanium-based fiber materials as well as carbon-based gas diffusion layers (GDL) are used in the different setups. To investigate the electrochemical behavior the test benches were operated with different electrochemical workstations and power potentiostats from Zahner-Elektrik GmbH & Co. KG, Germany. Using these devices, polarization curves and EIS were obtained in a current density range up to 7 A•cm⁻². The polarization curves were measured with a holding time of two minutes at each current density. The cells and electrochemical tests are summarized in Table 1.

3. Results and discussion

Low-frequency inductive loops are reproducible phenomena which occur in all of the PEMECs studied in the present work. Before testing, all CCMs were conditioned in a comparable way. The measurements shown in Fig. 1 were conducted at a temperature of 80 °C and pressure of 1 bar at Fraunhofer ISE and at ambient pressure at KIT IAM-ET. CCMs, testing environments and current densities were varied. In order to exclude the influence of drift and nonlinearities, the Kramers-Kronig test [32] was performed for all measurements and an example is shown for the measurement at 7 A•cm⁻². In most cases Kramers-Kronig residuals below 1% were observed, with only Fig. 1(c) showing high residuals at high frequencies, which are related to inductive artefacts due to wiring and the test cell housing. For the low-frequency region analyzed in this work, the Kramers-Kronig residuals are at an acceptable level.

A significant inductive loop is visible in all measurements shown in Fig. 1. Increasing the current density leads to a decrease in (positive) capacitive and an increase in (negative) inductive polarization resistance. With these results, we can show that this behavior is independent of the CCMs and PTLs, test cell housing and test benches used in this work.

Setups 1, 2 and 4 show quite similar polarization behavior and trends

with increasing current density. Furthermore, the frequency at which the low-frequency inductive behavior starts is very similar. Setups 3 and 4 show high-frequency inductance due to their wiring – here we refer to various publications for a more detailed understanding [28,33,34]. However, there are differences in the low-frequency region in the spectra of setup 3. An additional capacitive process most likely related to diffusion at frequencies of approximately 1 Hz can be seen. Therefore, the inductive behavior is only dominant at lower frequencies.

Meyer and Zhao described perturbation-induced inductive behavior at low frequencies in a PEMFC [12]. They oscillated the inlet air is oscillated in the same way as current density amplitude around the setpoint value and observed increasing inductive loops. In the case of the setups used in this study, analysis of the water inlet flow revealed (non-oscillating, chaotic) variations below 1%. These minor flow rate variations cannot create the observed inductive loops.

To understand the impact of this inductive behavior on cell performance we considered an example: we compared the polarization curve of setup 3 with the impedance spectra at different current densities, see Fig. 2. We determined the specific resistances, as the high-frequency series resistance (R_{Series}) and low-frequency resistance (R_{LFR}) using the intersections with $-\text{Im}(Z) = 0$ at high and medium frequencies in the spectra and the resistance at the minimal frequency of 10 mHz (minimal-frequency resistance, R_{MFR}). The resistance of the polarization curve (R_{DC}) was determined by calculating the local slope of the polarization curve at the investigated points (see Fig. 2a). To confirm that the inductive processes are affecting gas production, the measured volume flows of hydrogen and oxygen produced during the polarization curve are shown. At low flow rates (<20 Nml•min⁻¹) the flow meters are too imprecise to produce useful data. Between 1 A•cm⁻² and 8 A•cm⁻² a mean ratio between hydrogen and oxygen flow rate of 2.03 ± 0.06 was measured. With the most pessimistic evaluation (lowest value within the accuracy of the mass flow meters) the Faradaic efficiency was $\eta_{F,H_2} = 0.99 \pm 0.01$.

Fig. 2(b) shows the EIS at different current densities. The specific resistances are marked for the EIS at 7 A•cm⁻² to demonstrate the evaluation method, which was used for every operation point. The value of R_{DC} taken from the polarization curve is also indicated. Fig. 2(c) shows the resistances evaluated for current densities from 1 A•cm⁻² to 7 A•cm⁻². For a low current density of 1 A•cm⁻² the inductive behavior is small and so R_{LFR} and R_{MFR} are approximately similar to R_{DC} . With increasing current density these values start to diverge. At higher current densities R_{LFR} has a significantly higher value than R_{DC} . By contrast, R_{MFR} shows a similar trend to R_{DC} . The difference between R_{DC} and R_{MFR} is due to the fact that R_{MFR} is the resistance measured for the lowest frequency of $f = 10$ mHz corresponding to a time constant $\tau \cong 16$ s, whereas the delay time during the polarization curve measurement was 120 s. The extrapolation of the spectra towards lower frequencies indicates good agreement with R_{DC} . In the study of PEMFCs it has already been reported that R_{DC} can reach values lower than R_{LFR} [11,15]. In this case a part of the capacitive polarization loss is compensated by the low-

Table 1
Overview of different testing setups.

Setup	Test cell	CCM	PTL-anode	PTL-cathode	Test bench	Potentiostat	Operated flow rates	EIS frequency range
1	ISE reference cell	Commercial 1	PTL 1 (titanium-based fiber)	PTL 1 (titanium-based fiber)	ISE developed in-house	Zahner Zennium X + Zahner PP242	30 ml•min ⁻¹ •cm ⁻²	100 kHz – 100 mHz
2	ISE reference cell	Commercial 2	PTL 1 (coated titanium-based fiber)	GDL 1 (carbon paper)	ISE developed in-house	Zahner Zennium Pro + Zahner PP242	30 ml•min ⁻¹ •cm ⁻²	100 kHz – 100 mHz
3	Schaeffler EL10	Commercial 3	PTL 2 (coated titanium-based fiber)	GDL 2 (carbon paper)	Greenlight Innovation	Zahner Zennium X + 2 × PP241	4 ml•min ⁻¹ •cm ⁻²	100 kHz – 10 mHz
4	ISE AtC cell	Commercial 1	PTL 1 (titanium-based fiber)	PTL 1 (titanium-based fiber)	ISE developed in-house	Zahner Zennium X + Zahner EL1000 + third party power supply	13 ml•min ⁻¹ •cm ⁻²	5 kHz – 100 mHz

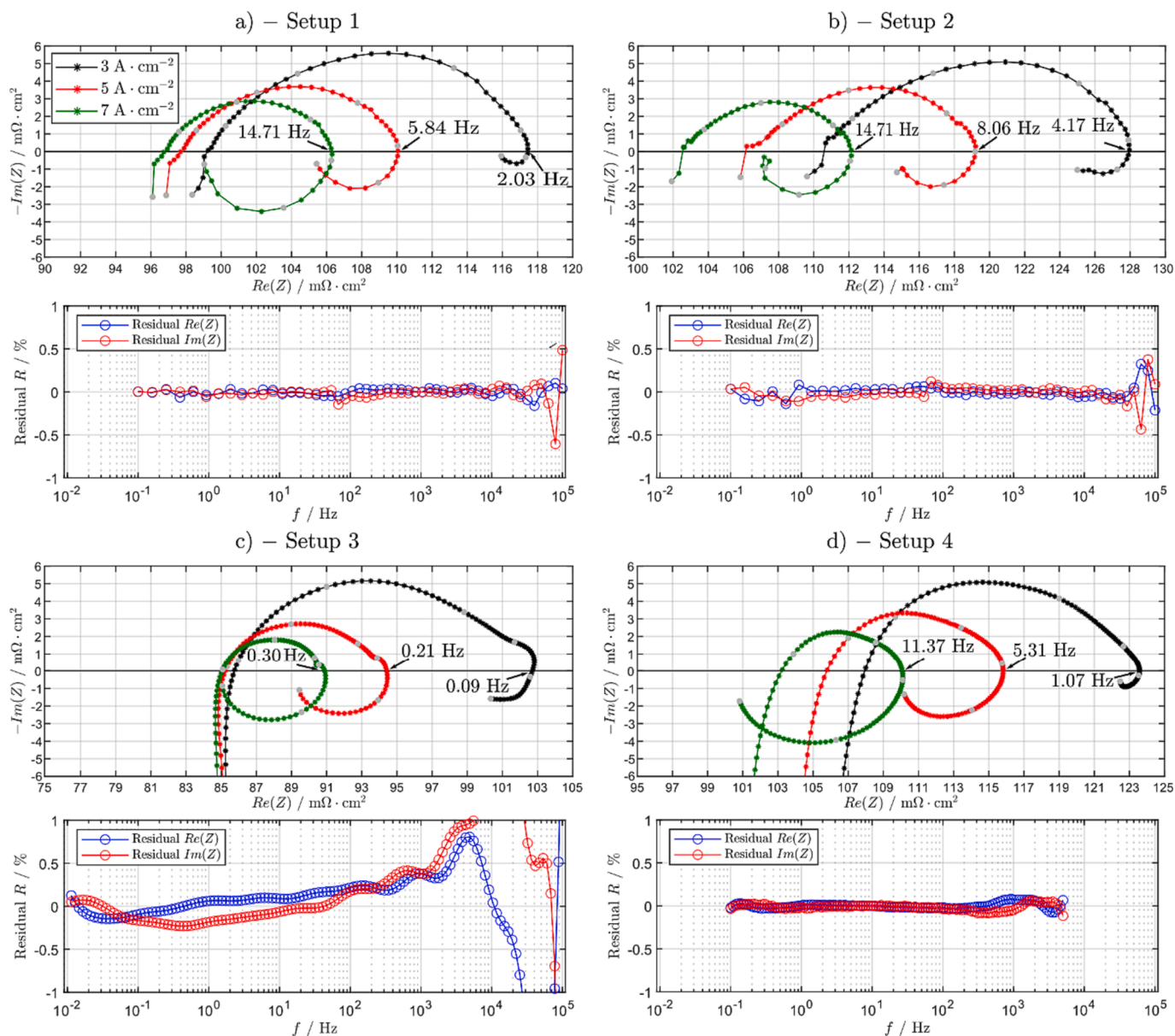


Fig. 1. Comparison of inductive loops for different test cell setups (1–4). As an example, the residual of the Kramers-Kronig test is shown for each measurement at $7 \text{ A}\cdot\text{cm}^{-2}$.

frequency inductive process. We show here that in PEMECs under extreme conditions, the R_{DC} has even lower values than the series resistance. The negative resistance of the low-frequency inductive processes not only fully compensates for the capacitive polarization resistance but additionally a significant part of the series resistance. It should be noted that the series resistance may not have been accurately determined due to high-frequency inductances as mentioned earlier. These might lead to an overestimation of the series resistance. Another explanation is that the measured series resistance is too high due to the fact that there are slow processes decreasing the membrane resistivity, which are only recognizable at low frequencies. Examples of this are different states of humidification due to slow water transport and changes in catalyst coverage as suggested for PEMFCs [15,17,35].

As well as the current density, temperature has a great influence on the inductive behavior. Fig. 3(a) shows the temperature variation of setup 1 with platinum-coated PTLs at $7 \text{ A}\cdot\text{cm}^{-2}$. The impact of the low-frequency inductive processes increases drastically with decreasing temperature. In Fig. 3(b) the magnitude of the capacitive polarization resistance ($R_{\text{Pol, CP}}$) is determined by taking the difference of the real part

of the impedance between R_{LFR} and R_{Series} . Analogously, $R_{\text{Pol, IP}}$ describes the magnitude of the real part of the inductive process determined between R_{MFR} and R_{LFR} . R_{Series} is determined using the intersection with $-\text{Im}(Z) = 0$ at high frequencies. R_{DC} is determined using the corresponding polarization curves of each measurement. Here we notice one or more inductive processes with a “negative resistance” that increase with decreasing temperature. By contrast, the capacitive loop at medium frequencies does not seem to be influenced by the temperature. This is quite surprising, since one usually associates the charge transfer resistance of the oxygen evolution reaction with this polarization loop, which increases significantly with decreasing temperature. One possible explanation for this is inaccuracies in the estimation of R_{Series} and R_{LFR} . Another reason for the seemingly steady charge transfer resistance is that diffusion processes, which also occur at these frequencies, superimpose charge transfer and lead to a more stable capacitive polarization with varying temperature. At frequencies $< 1 \text{ Hz}$ diffusion processes are usually dominant and detectable in the impedance spectra. We see here an additional but contrary process, which decreases the overpotentials occurring in this frequency range. It should be noted that the operational

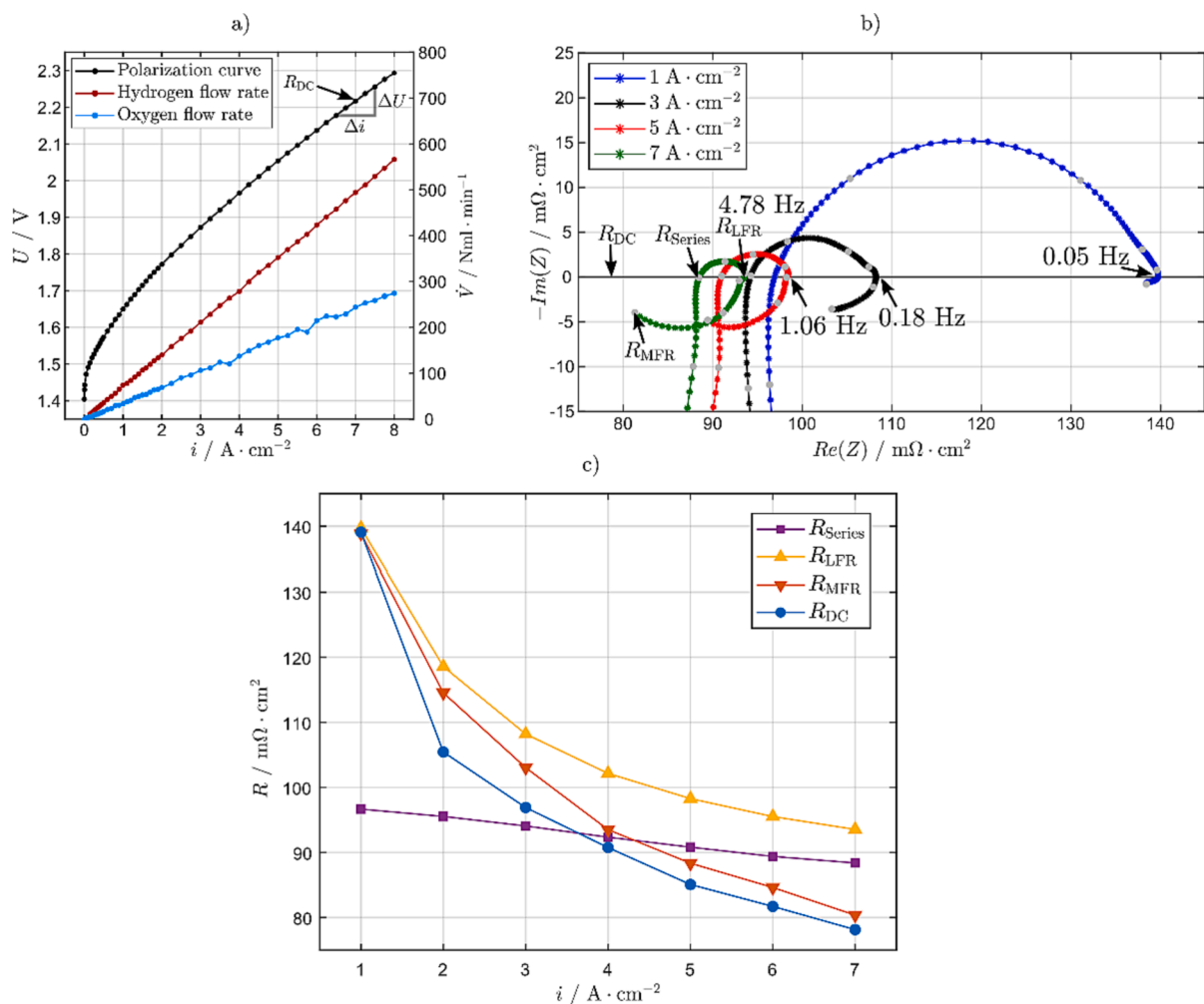


Fig. 2. (a) Polarization curve and produced hydrogen and oxygen standard flow rates of setup 3. (b) EIS of setup 3 at different current densities, ambient pressure and 60 °C. The specific resistances (R_{Series} , R_{LFR} and R_{MFR}) and the DC resistance R_{DC} , calculated from the local slope of the polarization curve (a), are shown as an example for the measurement at 7 A · cm⁻². (c) Specific resistances of the EIS and the polarization curve over the current density.

cell voltage increases with decreasing temperature, mostly related to an increase in membrane resistance. The voltage dependence might also be a reason for the increase in the inductive processes as, for example, in the potential-dependent state of catalyst coverage [15]. At extreme conditions, e.g. high current density and low temperature (7 A · cm⁻² at 40 °C), the inductive loop contributes up to three times as much to the total cell resistance as the capacitive loop, see Fig. 3(b).

4. Conclusion

In this article, we show that inductive behavior at low frequencies is an existing and reproducible phenomenon in PEM water electrolysis cells. This holds true for different CCMs and PTLs, test cell housings and test benches. The impact of inductive loops on the cell resistance increases towards higher current densities and lower temperatures.

It is demonstrated that the observed inductive low-frequency loops represent polarization phenomena exhibiting a negative resistance and thus improving cell performance. At high current densities this negative resistance might even exceed the positive polarization resistance originating from conventional capacitive polarization phenomena in the cell. Hence, inductive low-frequency processes should be considered in performance evaluation as they might significantly increase cell performance. We believe that focusing on increasing the inductive process is as important as reducing the capacitive process at low frequencies.

The inductive behavior at low frequencies should be considered in

further EIS-based investigations of PEMECs. A physicochemical understanding and modeling of the related processes is essential for simulation studies and model-based cell optimization. This behavior will become even more important in view of the desire to operate PEMECs at higher current densities.

CRediT authorship contribution statement

Niklas Hensle: Conceptualization, Methodology, Validation, Formal analysis, Investigation, Writing – original draft, Visualization, Project administration. **Debora Brinker:** Conceptualization, Methodology, Validation, Formal analysis, Investigation, Writing – original draft, Visualization, Project administration. **Sebastian Metz:** Conceptualization, Writing – review & editing, Supervision, Funding acquisition. **Tom Smolinka:** Conceptualization, Writing – review & editing, Supervision, Funding acquisition. **André Weber:** Conceptualization, Writing – review & editing, Supervision, Funding acquisition.

Declaration of Competing Interest

The authors declare that they have no known competing financial interests or personal relationships that could have appeared to influence the work reported in this paper.

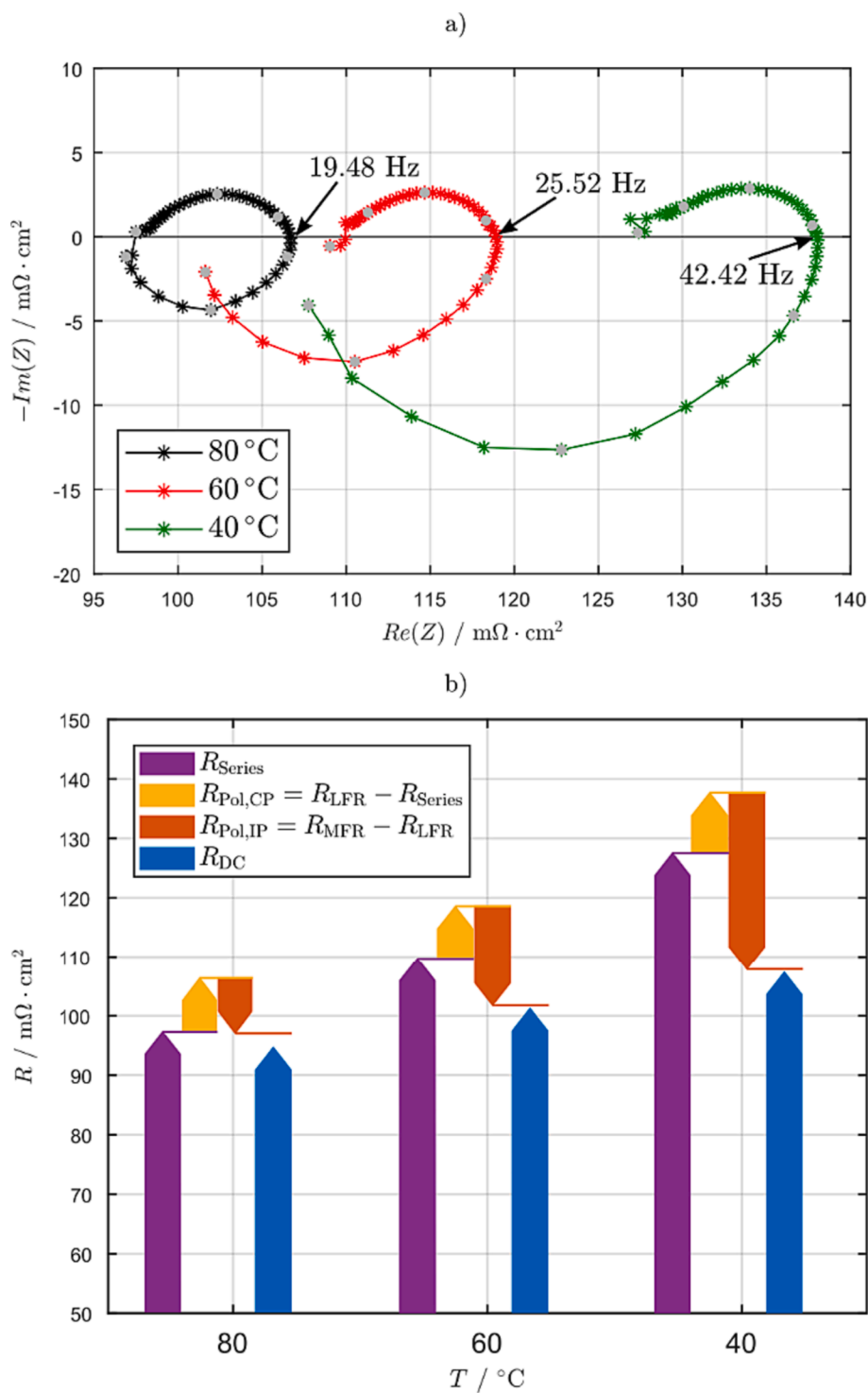


Fig. 3. (a) Temperature variation of EIS of setup 1 with platinum-coated PTLs at $7 \text{ A} \cdot \text{cm}^{-2}$. (b) Evaluation of the magnitude of the series resistance, the capacitive and inductive polarization resistance obtained by EIS and the DC resistance evaluated from the polarization curve.

Data availability

Data will be made available on request.

Acknowledgements

The authors gratefully acknowledge funding from the Federal Ministry of Education and Research, Germany (BMBF 03HY103C and 03HY103F). We thank Schaeffler Technologies AG & Co. KG, Germany

for the collaboration. Charlotte Menke is acknowledged for her support in carrying out the measurements at Fraunhofer ISE. We thank Dietmar Gerteisen for the profound discussion.

References

- [1] Q.-C. Zhuang, X.-Y. Qiu, S.-D. Xu, Y.-H. Qiang, S.-G. Sun, in Dr. Ilias Belharouak (Ed.), *Lithium Ion Batteries – New Developments*, ISBN: 978-953-51-0077-5, InTech, 2012. <https://doi.org/10.5772/26749>.

- [2] H. Brandstätter, I. Hanzu, M. Wilkening, *Electrochim. Acta* 207 (2016) 218–223, <https://doi.org/10.1016/j.electacta.2016.03.126>.
- [3] J.S. Gnanaraj, R.W. Thompson, S.N. Iaconatti, J.F. DiCarlo, K.M. Abraham, *Electrochem. Solid-State Lett.* 8 (2005) A128, <https://doi.org/10.1149/1.1850390>.
- [4] A. Barbucci, R. Bozzo, G. Cerisola, P. Costamagna, *Electrochim. Acta* 47 (2002) 2183–2188, [https://doi.org/10.1016/S0013-4686\(99\)00134-6](https://doi.org/10.1016/S0013-4686(99)00134-6).
- [5] K. Chen, N. Ai, S.P. Jiang, *Solid State Ionics* 291 (2016) 33–41, <https://doi.org/10.1016/j.ssi.2016.04.021>.
- [6] K. Kreka, K.V. Hansen, M.B. Mogensen, K. Norrman, C. Chatzichristodoulou, T. Jacobsen, *J. Electrochem. Soc.* 165 (2018) F253–F263, <https://doi.org/10.1149/2.0141805jes>.
- [7] D. Montinaro, A.R. Contino, A. Dellai, M. Rolland, *Int. J. Hydrogen Energy* 39 (2014) 21638–21646, <https://doi.org/10.1016/j.ijhydene.2014.09.081>.
- [8] H. Sumi, H. Shimada, K. Watanabe, Y. Yamaguchi, K. Nomura, Y. Mizutani, Y. Okuyama, *ACS Appl. Energy Mater.* 6 (2023) 1853–1861, <https://doi.org/10.1021/acsaem.2c03733>.
- [9] S.K. Roy, M.E. Orazem, B. Tribollet, *J. Electrochem. Soc.* 154 (2007) B1378, <https://doi.org/10.1149/1.2789377>.
- [10] S.K. Roy, M.E. Orazem, *J. Electrochem. Soc.* 154 (2007) B883, <https://doi.org/10.1149/1.2747533>.
- [11] I. Pivac, F. Barbir, *J. Power Sources* 326 (2016) 112–119, <https://doi.org/10.1016/j.jpowsour.2016.06.119>.
- [12] Q. Meyer, C. Zhao, *J. Power Sources* 488 (2021), 229245, <https://doi.org/10.1016/j.jpowsour.2020.229245>.
- [13] B.P. Setzler, T.F. Fuller, *J. Electrochem. Soc.* 162 (2015) F519–F530, <https://doi.org/10.1149/2.0361506jes>.
- [14] D. Klotz, *Electrochem. Commun.* 98 (2019) 58–62, <https://doi.org/10.1016/j.elecom.2018.11.017>.
- [15] C. Gerling, M. Hanauer, U. Berner, K.A. Friedrich, *J. Electrochem. Soc.* 170 (2023) 14504, <https://doi.org/10.1149/1945-7111/acb3ff>.
- [16] A. Schiefer, M. Heinzmann, A. Weber, *Fuel Cells* 20 (4) (2020) 499–506, <https://doi.org/10.1002/face.201900212>.
- [17] S. Cruz-Manzo, P. Greenwood, *J. Electroanal. Chem.* 900 (2021), 115733, <https://doi.org/10.1016/j.jelechem.2021.115733>.
- [18] O. Antoine, Y. Bultel, R. Durand, *J. Electroanal. Chem.* 499 (2001) 85–94, [https://doi.org/10.1016/S0022-0728\(00\)00492-7](https://doi.org/10.1016/S0022-0728(00)00492-7).
- [19] H. Kuhn, A. Wokaun, G.G. Scherer, *Electrochim. Acta* 52 (2007) 2322–2327, <https://doi.org/10.1016/j.electacta.2006.03.108>.
- [20] C.A. Schiller, H. Goehr, *Z. Phys. Chem.* 148 (1986) 105–124, <https://doi.org/10.1524/zpch.1986.148.1.105>.
- [21] C.A. Schiller, F. Richter, E. Gülzow, N. Wagner, *Phys. Chem. Chem. Phys.* 3 (2001) 2113–2116, <https://doi.org/10.1039/B007674K>.
- [22] N. Wagner, E. Gülzow, *J. Power Sources* 127 (2004) 341–347, <https://doi.org/10.1016/j.jpowsour.2003.09.031>.
- [23] J. van der Merwe, K. Uren, G. van Schoor, D. Bessarabov, *Int. J. Hydrogen Energy* 39 (2014) 14212–14221, <https://doi.org/10.1016/j.ijhydene.2014.02.096>.
- [24] M. Suermann, A. Pătru, T.J. Schmidt, F.N. Büchi, *Int. J. Hydrogen Energy* 42 (2017) 12076–12086, <https://doi.org/10.1016/j.ijhydene.2017.01.224>.
- [25] S. Siracusano, S. Trocino, N. Briguglio, V. Baglio, A.S. Aricò, *Materials (Basel)* 11 (2018) 1368, <https://doi.org/10.3390/ma11081368>.
- [26] J.C. Garcia-Navarro, M. Schulze, K.A. Friedrich, *J. Power Sources* 431 (2019) 189–204, <https://doi.org/10.1016/j.jpowsour.2019.05.027>.
- [27] I. Dedigama, P. Angeli, K. Ayers, J.B. Robinson, P.R. Shearing, D. Tsaoulidis, D. Brett, *Int. J. Hydrogen Energy* 39 (2014) 4468–4482, <https://doi.org/10.1016/j.ijhydene.2014.01.026>.
- [28] I. Franzetti, A. Pushkarev, A.-L. Chan, T. Smolinka, *Energy Technol.* (2023), ente.202300375. <https://doi.org/10.1002/ente.202300375>.
- [29] T. Ferriday, P.H. Middleton, *Int. J. Hydrogen Energy* 44 (2019) 27656–27663, <https://doi.org/10.1016/j.ijhydene.2019.09.020>.
- [30] Fraunhofer Institute for Solar Energy Systems ISE, Annual Report 2020/21.
- [31] T. Lickert, M.L. Kiermaier, K. Bromberger, J. Ghinaiya, S. Metz, A. Fallisch, T. Smolinka, *Int. J. Hydrogen Energy* 45 (2020) 6047–6058, <https://doi.org/10.1016/j.ijhydene.2019.12.204>.
- [32] M. Schönleber, D. Klotz, E. Ivers-Tiffée, *Electrochim. Acta* 131 (2014) 20–27, <https://doi.org/10.1016/j.electacta.2014.01.034>.
- [33] I.V. Pushkareva, M.A. Solovyev, S.I. Butrim, M.V. Kozlova, D.A. Simkin, A. S. Pushkarev, *Membranes (Basel)* 13 (2023) 192, <https://doi.org/10.3390/membranes13020192>.
- [34] E.-C. Shin, P.-A. Ahn, H.-H. Seo, J.-M. Jo, S.-D. Kim, S.-K. Woo, J.H. Yu, J. Mizusaki, J.-S. Lee, *Solid State Ionics* 232 (2013) 80–96, <https://doi.org/10.1016/j.ssi.2012.10.028>.
- [35] A. Kulikovskiy, *Electrochem. Commun.* 140 (2022), 107340, <https://doi.org/10.1016/j.elecom.2022.107340>.